

This is the accepted manuscript made available via CHORUS. The article has been published as:

Heavy quark diffusion in strong magnetic fields at weak coupling and implications for elliptic flow

Kenji Fukushima, Koichi Hattori, Ho-Ung Yee, and Yi Yin

Phys. Rev. D **93**, 074028 — Published 20 April 2016

DOI: [10.1103/PhysRevD.93.074028](https://doi.org/10.1103/PhysRevD.93.074028)

Heavy Quark Diffusion in Strong Magnetic Fields at Weak Coupling and Implication to Elliptic Flow

Kenji Fukushima^{1*}, Koichi Hattori^{2,3†}, Ho-Ung Yee^{4,2‡} and Yi Yin^{5§}

¹ *Department of Physics, The University of Tokyo, 7-3-1 Bunkyo-ku, Hongo, Tokyo 113-0033, Japan*

² *RIKEN-BNL Research Center, Brookhaven National Laboratory, Upton, New York 11973-5000, U.S.A.*

³ *Nishina Center, RIKEN, Wako, Saitama 351-0198, Japan*

⁴ *Department of Physics, University of Illinois, Chicago, Illinois 60607, U.S.A.*

⁵ *Brookhaven National Laboratory, Upton, New York 11973-5000, U.S.A.*

March 3, 2016

Abstract

We compute the momentum diffusion coefficients of heavy quarks, κ_{\parallel} and κ_{\perp} , in a strong magnetic field B along the directions parallel and perpendicular to B , respectively, at the leading order in QCD coupling constant α_s . We consider a regime relevant for the relativistic heavy ion collisions, $\alpha_s eB \ll T^2 \ll eB$, so that thermal excitations of light quarks are restricted to the lowest Landau level (LLL) states. In the vanishing light-quark mass limit, we find $\kappa_{\perp}^{\text{LO}} \propto \alpha_s^2 T eB$ in the leading order that arises from screened Coulomb scatterings with (1+1)-dimensional LLL quarks, while κ_{\parallel} gets no contribution from the scatterings with LLL quarks due to kinematic restrictions. We show that the first non-zero leading order contributions to $\kappa_{\parallel}^{\text{LO}}$ come from the two separate effects: 1) the screened Coulomb scatterings with thermal gluons, and 2) a finite light-quark mass m_q . The former leads to $\kappa_{\parallel}^{\text{LO, gluon}} \propto \alpha_s^2 T^3$ and the latter to $\kappa_{\parallel}^{\text{LO, massive}} \propto \alpha_s (\alpha_s eB)^{1/2} m_q^2$. Based on our results, we propose a new scenario for the large value of heavy-quark elliptic flow observed in RHIC and LHC. Namely, when $\kappa_{\perp} \gg \kappa_{\parallel}$, an anisotropy in drag forces gives rise to a sizable amount of the heavy-quark elliptic flow even if heavy quarks do not fully belong to an ellipsoidally expanding background fluid.

*e-mail: fuku@nt.phys.s.u-tokyo.ac.jp

†e-mail: koichi.hattori@riken.jp

‡e-mail: hyee@uic.edu

§e-mail: yyin@bnl.gov

1 Introduction

Heavy ion collisions create Quark-Gluon Plasma (QGP) in the presence of strong electromagnetic fields produced by charged constituents of colliding nuclei [1, 2, 3, 4]. When the collision is non-central with a finite impact parameter, spectator protons produce a net magnetic field whose initial strength could be comparable to the pion mass scale $eB \geq m_\pi^2$. Experimental consequences from those enormous magnetic fields have attracted much attention of theoretical studies (see Refs. [5, 6, 7, 8] for recent reviews). One particular example is the chiral magnetic effect (CME) [9] from the interplay of the magnetic field and the quantum anomaly that has been predicted to induce charge separation. Closely related to CME, it has been argued that the chiral magnetic wave [10, 11] would cause an electric quadrupole moment leading to charge-dependent elliptic flow [12, 13]. Meanwhile, as attempts to seek for a signature of such strong B with/without local parity violation, possible enhanced anisotropic production of photons and dileptons has been investigated in literature [14, 15, 16, 17, 18, 19, 20, 21].

Whether the magnetic field leaves observable effects in heavy ion collisions depends on several key properties in the early stage of QGP. One of the crucial but still open questions is the thermalization of light quarks in QGP that can potentially induce a sizable electric conductivity. If the electric conductivity is large enough, decaying magnetic field would lead to an induced current and this current would elongate the lifetime of the magnetic field consistently with Lenz's law [22, 23, 24]. In turn, the strong magnetic field may also affect QGP thermalization processes via coupling to the light quarks, i.e., quark production rate should depend on external electromagnetic fields [25, 26, 27]. With these open questions in mind, exploring and studying observables which are sensitive to the existence of magnetic field would be important, paving the way towards calibrating the strength and lifetime of magnetic field and understanding interesting properties of QGP with the magnetic field.

In this work, we consider one of such important probes, namely, dynamics of heavy quarks. So far, several studies on magnetic field effects have been carried out for *static* properties of open heavy flavors [28, 29, 30] and of quarkonia [31, 32, 33, 34, 35, 36, 37, 38] *. The measurements of open heavy flavors and quarkonia in Relativistic Heavy Ion Collider (RHIC) and Large Hadron Collider (LHC), however, have indicated the importance of *dynamical* properties in the real-time evolution inside the created matter,

*In contrast, by “dynamical” properties we mean real-time processes in a hot and dense medium.

that is, transport and thermalization of heavy flavors in the QGP [39, 40, 41, 42, 43] (see also Ref. [44] for a recent review and references therein). This motivates us to study heavy quark dynamics in QGP in the presence of a strong magnetic field and to compute transport coefficients that control the drag force and the time scale of thermalization of heavy quarks. See Ref.[45] for a recent computation of heavy quark drag force in AdS/CFT correspondence with a *weak*, linearized magnetic field.

As in the previous studies of heavy quark diffusion without magnetic field [39, 46], we use weak coupling perturbative QCD techniques to compute the heavy quark diffusion constant in leading order (LO) of strong coupling constant α_s . The heavy quark mass M_Q is assumed to be much larger than the scale of the magnetic field; $M_Q \gg \sqrt{eB}$, which is a good assumption for charm and bottom quarks, so the heavy quark motions are not directly affected by magnetic fields[†].

At finite temperature, there exist thermally populated light quarks and gluons that can scatter with the heavy quark, which gives random momentum kicks to diffuse the heavy quark momentum. At LO in α_s these scatterings are mediated by one-gluon exchange and the scatterers can be regarded as quasi-particles in thermally equilibrated matter. For magnetic field $eB \sim T^2$, it would put the light quark dispersion relation into the Landau quantized ones (i.e. Landau levels, which will be abbreviated as LL below) in thermal equilibrium, which will affect both the scattering quark spectrum and its screening effect on the one-gluon mediation via the gluon self-energy from quark loops. We will show that the gluon screening mass (that is, the Debye mass) from the Landau quantized quark 1-loop is $m_{D,B}^2 \sim \alpha_s eB$, whereas the one from the gluon 1-loop is $\alpha_s T^2$ as usual which is suppressed compared to the former quark contribution. Therefore, we include the screening mass $m_{D,B}^2$ into the Coulomb scattering diagram between the heavy quark and thermal scatterers, which is necessary for regularize the infrared regime in the soft gluon exchanges.

The thermal masses of scatterers, i.e., time-like gluons and LLL quarks, have the same order as $m_{D,B}^2$. However, since the typical momenta of scattering quarks and gluons are hard $\sim T$, we assume that the self-energy corrections to these hard LLL quarks and gluons in the present leading-order calculation can be neglected, which specifies a

[†]More precisely, the thermal velocity of heavy quark is $|\mathbf{v}| \sim \sqrt{T/M_Q}$, and the Lorentz force is $(d\mathbf{p}/dt)_{\text{Lorentz}} = e\mathbf{v} \times \mathbf{B}$ which is suppressed as $\sim eB\sqrt{T/M_Q}$ for large M_Q . On the other hand, we will see that the momentum kicks from thermal scattering with light quarks and gluons that we compute at LO in this work are not suppressed for large M_Q .

hierarchy $\alpha_s eB \ll T^2$. Note also that, in this regime, one can neglect the self-energy corrections to the hard thermal particles which compose the internal lines of the gluon self-energy diagrams, so that the screening mass $m_{D,B}^2$ mentioned above can be obtained from the simple one-loop calculation.

Although the description of the case of $eB \sim T^2$ should involve all the LLs of thermally equilibrated light quarks (for the calculation of the self-energy with all LLs; see Refs. [47, 48, 49]), we instead consider an extreme limit of strong magnetic field $eB \gg T^2$ so that only the LLL states are thermally occupied. This allows us to obtain some analytic results that are helpful to unravel the key physics. Thus, in this work, the regime of our interest is specifically given as $\alpha_s eB \ll T^2 \ll eB$, and the higher LL occupations are exponentially suppressed by powers of $e^{-\sqrt{eB}/T}$. In realistic heavy ion collisions, these inequalities are approximately satisfied.

Our main finding is that in the presence of strong magnetic field, the drag forces or the momentum diffusion coefficients become highly anisotropic. In particular, the ratio between the longitudinal momentum diffusion coefficient κ_{\parallel} and the transverse one κ_{\perp} becomes

$$\frac{\kappa_{\parallel}}{\kappa_{\perp}} \sim \frac{T^2}{eB} \ll 1, \quad (1.1)$$

in the regime we are working on. We will discuss the phenomenological implication of (1.1) to heavy flavor elliptic flow and will propose a new scenario for the sizable elliptic flow of heavy quarks observed in experiments: a strong magnetic field would enhance the heavy flavor elliptic flow even without thermalization of heavy quarks with respect to the expanding plasma, which is in favor of resolving the heavy-flavor puzzle triggered by the elliptic flow measurement of the D mesons.

This paper is organized as follows. In Section 2 we introduce the basic formulation of how to compute the momentum diffusion coefficients, κ_{\parallel} and κ_{\perp} , describing the in-medium heavy quark motion. At LO we express those transport coefficients using the Coulomb scattering rate in terms of the longitudinal gluon spectral function. We then perform our explicit calculations of the spectral function in Section 3. We present the results in the zero quark mass limit in Section 4 and find $\kappa_{\perp} \sim \alpha_s^2 eBT$, while κ_{\parallel} does not get such a contribution due to kinematic constraints. To find the first non-vanishing contribution to κ_{\parallel} , we then proceed to the hard gluon scattering contribution and also the finite mass corrections in Section 5. In Section 6, we discuss the phenomenological implication of our results to a non-thermal origin of the heavy quark elliptic flow induced by strong magnetic field. We conclude in Section 7.

2 Random Forces and Diffusion Coefficients

As a preparation for our computations in the subsequent sections, let us here summarize the basic formalism for the heavy quark transports. Heavy quarks in a finite temperature plasma are subject to random kicks from thermally excited light quarks and gluons, and their motions are described by Langevin equations [39]:

$$\frac{dp_z}{dt} = -\eta_{\parallel} p_z + \xi_z, \quad \frac{d\mathbf{p}_{\perp}}{dt} = -\eta_{\perp} \mathbf{p}_{\perp} + \boldsymbol{\xi}_{\perp}. \quad (2.2)$$

Since the external magnetic field provides a preferred spatial direction, we have a set of two equations for the heavy quark motions, parallel and perpendicular to the magnetic field that is oriented in the z -direction. In Eq. (2.2), p_z and \mathbf{p}_{\perp} denote the heavy quark momenta parallel and perpendicular to the magnetic field respectively, and the random forces, ξ_z and $\boldsymbol{\xi}_{\perp}$, as well as the drag coefficients, η_{\parallel} and η_{\perp} , should be defined separately for parallel and perpendicular directions to the magnetic field. The random forces are assumed to be white noises:

$$\langle \xi_z(t) \xi_z(t') \rangle = \kappa_{\parallel} \delta(t - t'), \quad \langle \xi_{\perp}^i(t) \xi_{\perp}^j(t') \rangle = \kappa_{\perp} \delta^{ij} \delta(t - t') \quad (i, j = x, y), \quad (2.3)$$

and these coefficients, κ_{\parallel} and κ_{\perp} , are related to the drag coefficients, η_{\parallel} and η_{\perp} , through the fluctuation-dissipation theorem as

$$\eta_{\parallel} = 2M_Q T \kappa_{\parallel}, \quad \eta_{\perp} = 2M_Q T \kappa_{\perp}. \quad (2.4)$$

We will compute anisotropic momentum diffusion coefficients, κ_{\parallel} and κ_{\perp} , in the presence of magnetic field.

The above Langevin picture as well as the separation between longitudinal and transverse dynamics can be justified for a sufficiently large $M_Q \gg eB/T$. To see this, we should note that the typical thermal momentum of heavy quark is of the order of $\sqrt{M_Q T}$, and its typical velocity is $|\mathbf{v}| \sim \sqrt{T/M_Q}$. We will see in the following sections that the typical momentum transfer $q_{\perp} = |\mathbf{q}_{\perp}|$ from the LLL quarks to the heavy quark in the LO computation ranges in $\sqrt{\alpha_s eB} \lesssim q_{\perp} \lesssim \sqrt{eB}^{\dagger}$ and that the typical momentum transfer from thermal gluons at LO ranges in $\sqrt{\alpha_s eB} \lesssim |\mathbf{q}| \lesssim T \ll \sqrt{eB}$. Therefore, for $M_Q \gg eB/T \gg T$, the momentum transfer in each scattering is small compared to the thermal momentum, and it involves many scatterings to change the heavy quark momentum significantly. Then, the description of heavy quark motion should become statistical,

[†]This latter inequality can be expected immediately from the size of the LLL wavefunction $\sim 1/\sqrt{eB}$ that is the inverse of the typical transverse momentum.

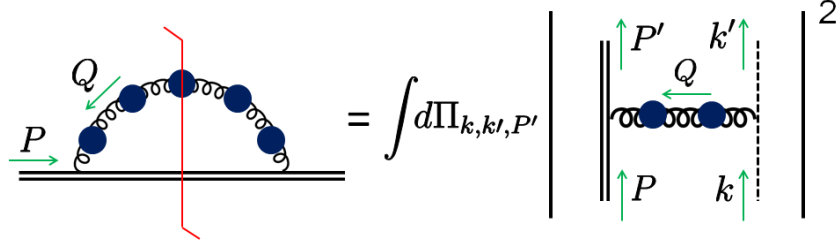


Figure 1: Momentum diffusion of a heavy quark (double line) due to Coulomb scatterings with thermal quarks and gluons (collectively denoted as a dashed line).

leading to the above Langevin dynamics. The same conclusion can be obtained also by the condition that the energy transfer ω in each collision should be much smaller than the temperature, in order for the fluctuation-dissipation relation from the equi-partition theorem to be meaningful, that is, $\omega \sim |\mathbf{v} \cdot \mathbf{q}| \sim \sqrt{T/M_Q} \cdot \sqrt{eB} \ll T$ holds when $M_Q \gg eB/T$. The separation between the transverse and the longitudinal dynamics in Eq. (2.2) simply follows from that the mixed coefficient $\kappa_{\perp z}$ should be proportional to the transverse velocity \mathbf{v}_{\perp} from rotational symmetry, which are of higher order in small velocity limit $|\mathbf{v}| \sim \sqrt{T/M_Q} \ll 1$.

The momentum diffusion coefficients are equivalently defined by

$$\kappa_{ij} \equiv \lim_{\Delta t \rightarrow 0} \frac{1}{\Delta t} \langle \Delta p_i \Delta p_j \rangle, \quad (2.5)$$

where $\Delta p^i = p^i(t + \Delta t) - p^i(t)$, and these are interesting transport coefficients of the QGP medium. They can be defined in a gauge invariant and non-perturbative way as [50]

$$\kappa_{ij} = \lim_{\omega \rightarrow 0} \frac{4\pi\alpha_s}{d_H} \int_{-\infty}^{+\infty} dt e^{i\omega t} \text{tr} \langle W(0, t) E_i(t) W(t, 0) E_j(0) \rangle, \quad (2.6)$$

where E_i and W are the chromoelectric field and the Wilson line in the heavy quark color representation, respectively. At LO in α_s the Wilson line is trivial and we can replace E_i with $\partial^i A^0$ in the static limit of $\omega \rightarrow 0$. The dimension of the heavy quark representation d_H is canceled by taking the trace in color space, resulting in Casimir C_R^{HQ} given by $C_R^{\text{HQ}} = (N_c^2 - 1)/(2N_c)$ and N_c , respectively, for heavy quarks in the fundamental and the adjoint representations. Thus, we need to evaluate the color diagonal part of the Wightman function of A^0 field, which is denoted as $G^{>00}$. In momentum representation spatial derivatives translate into momenta, leading to

$$\kappa_{ij} = \lim_{\omega \rightarrow 0} 4\pi\alpha_s C_R^{\text{HQ}} \int \frac{d^3\mathbf{q}}{(2\pi)^3} G^{>00}(\omega, \mathbf{q}) q_i q_j, \quad (2.7)$$

and from rotational symmetry, we have

$$\kappa_{\parallel} = \int d^3\mathbf{q} \frac{d\Gamma(\mathbf{q})}{d^3\mathbf{q}} q_z^2, \quad \kappa_{\perp} = \frac{1}{2} \int d^3\mathbf{q} \frac{d\Gamma(\mathbf{q})}{d^3\mathbf{q}} \mathbf{q}_{\perp}^2, \quad (2.8)$$

where

$$\frac{d\Gamma(\mathbf{q})}{d^3\mathbf{q}} \equiv \frac{4\pi\alpha_s}{(2\pi)^3} C_R^{\text{HQ}} \lim_{\omega \rightarrow 0} G^{>00}(\omega, \mathbf{q}) = \frac{4\pi\alpha_s}{(2\pi)^3} C_R^{\text{HQ}} \lim_{\omega \rightarrow 0} \frac{T}{\omega} \rho_L(\omega, \mathbf{q}), \quad (2.9)$$

can be interpreted as the scattering rate of the heavy quark via 1-gluon exchange with thermal particles per unit volume of momentum transfer \mathbf{q} . The ρ_L is the longitudinal gluon spectral density and in the last equality we used a thermal relation $G^{>00}(\omega) = n_B(\omega)\rho_L(\omega)$ which can be expanded as $G^{>00}(\omega) \approx (T/\omega)\rho_L(\omega)$ for $\omega \ll T$.

This interpretation of $d\Gamma(\mathbf{q})/d^3\mathbf{q}$ can be clearly seen in the heavy quark damping rate, which is given by the imaginary part of the heavy-quark self-energy from 1-gluon loop as in Fig. 1, that is the damping rate can be shown to be given by

$$\gamma^{\text{HQ}} = \int d^3\mathbf{q} \frac{d\Gamma(\mathbf{q})}{d^3\mathbf{q}}, \quad (2.10)$$

with the same definition of $d\Gamma(\mathbf{q})/d^3\mathbf{q}$ as above. We have $\rho_L = -2\text{Im}G_R^{00}$ and the expression (2.9), by cutting rules, describes the Coulomb scattering between thermal particles and the heavy quark at rest as shown in Fig. 1. The one-gluon mediation is generally screened by thermal self-energies (blobs in Fig. 1) to have IR divergences tamed. The screening is provided by contributions of both the LLL quark states and the HTL gluons, which will be detailed in the next section. In the case of $eB \gg T^2$ the LLL contribution to the screening mass ($m_D^2 \sim \alpha_s eB$) will dominate over the gluonic contribution ($\sim \alpha_s T^2$). As a wrap-up, we emphasize that the time-like region, $\omega^2 - |\mathbf{q}|^2 > 0$, of the spectral density $\rho_L(\omega, \mathbf{q})$ does not contribute to the momentum diffusion coefficients or the scattering rate (2.9) in the $\omega \rightarrow 0$ limit.

3 Formalism for computation of scattering rates

As discussed in the previous section, to compute the heavy quark diffusion and drag coefficients at LO, we need the longitudinal spectral density $\rho_L(\omega, \mathbf{q})$ near $\omega \rightarrow 0$, which can be obtained from the retarded gluon correlator $G_R^{00}(\omega, \mathbf{q})$. To include both the screening effects from and the scatterings with thermal particles, the one-loop gluon self-energy is re-summed into the longitudinal propagator $G_R^{00}(\omega, \mathbf{q})$. Roughly speaking, the real part of this self-energy gives the screening effects, while the imaginary part is responsible for the

spectrum of scattering particles. Fermions (i.e. light quarks) and hard thermal gluons will contribute to the self-energy, and we denote them as $\Pi_{R,\text{fermion}}^{\mu\nu}$ and $\Pi_{R,\text{gluon}}^{\mu\nu}$, respectively, throughout this paper. We first present our computation for $\Pi_{R,\text{fermion}}^{\mu\nu}$ in the LLL approximation as shown in Fig. 2. We investigate general features of the gluon self-energy due to the polarization of quarks and antiquarks in the LLL states in the next subsection 3.1 and express the resulting spectral density from it in subsection 3.2. The thermal gluon contribution to the self-energy, $\Pi_{R,\text{gluon}}^{\mu\nu}$, will be addressed later in section 5.2.

3.1 Gluon self-energy from quark loop

The two-point functions and the self-energy are diagonal in color indices, and so we factor them out for notational brevity. After taking the color trace, contributions from a particle species in the representation R to the one-loop self-energy is proportional to the following pre-factor,

$$T_R \equiv \frac{C_R^{\text{LQ}} \cdot \text{Dim}(R)}{\text{Dim}(G)}, \quad (3.11)$$

where $\text{Dim}(G) = N_c^2 - 1$ is the dimension of the adjoint representation and C_R^{LQ} is the light-quark Casimir. We have $T_R = 1/2$ and N_c for the fundamental and the adjoint representations, respectively. These factors take care of the color representation of light particles inside the loop.

We will utilize the real-time Schwinger-Keldysh formalism in “ra”-basis. In this language, we can express the retarded gluon self-energy as

$$\Pi_{R,\text{fermion}}^{\mu\nu}(Q) = i4\pi\alpha_s T_R \langle J_r^\mu(Q) J_a^\nu(-Q) \rangle, \quad (3.12)$$

where $J_{r,a}^\mu$ is the current operator (with color indices amputated as described before) and the subscript (r,a) refers to the Keldysh basis. Re-summing insertions of the external magnetic field (see Fig. 2), the real-time quark propagators at finite T in the LLL approximation are given by (see, e.g., Ref. [51] for an explicit construction of the quark propagator with B)

$$S_{ra}(p) = i e^{-\mathbf{p}_\perp^2 / |q_f e B|} \frac{2(\not{p}_\parallel + m_q) \mathcal{P}_-}{p_\parallel^2 - m_q^2} \Big|_{p^0 \rightarrow p^0 + i\epsilon}, \quad (3.13)$$

$$S_{ar}(p) = i e^{-\mathbf{p}_\perp^2 / |q_f e B|} \frac{2(\not{p}_\parallel + m_q) \mathcal{P}_-}{p_\parallel^2 - m_q^2} \Big|_{p^0 \rightarrow p^0 - i\epsilon}, \quad (3.14)$$

$$S_{rr}(p) = \left[\frac{1}{2} - n_F(p^0) \right] [S_{ra}(p) - S_{ar}(p)] \equiv \left[\frac{1}{2} - n_F(p^0) \right] \rho_F(p), \quad (3.15)$$

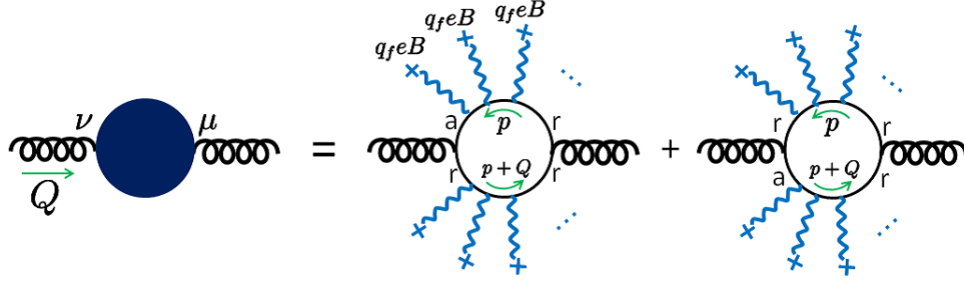


Figure 2: One-loop gluon self-energy due to the polarization of a pair of quark and antiquark LLL states. Indices “a” and “r” denote the Schwinger-Keldysh basis.

where q_f is the electric charge of quark species f in unit of e , and the magnetic field is assumed to be oriented in the z -direction. The metric in the longitudinal two-dimensional subspace is defined by $g_{\parallel}^{\mu\nu} = \text{diag}(1, 0, 0, -1)$, so that $p_{\parallel}^{\mu} = g_{\parallel}^{\mu\nu} p_{\nu}$ and $\not{p}_{\parallel} = p^0 \gamma^0 - p^z \gamma^z$. The spin-projection operators are defined by $\mathcal{P}_{\pm} \equiv (1 \pm i \text{sgn}(q_f B) \gamma^x \gamma^y)/2$, which project quark fields onto the 1+1 dimensional spinors. Note that these operators depend on the quark charge q_f since the spin magnetic moment depends on the quark charge. Nevertheless, our final result for κ will be independent of the sign of $q_f B$ because of the charge-conjugation invariance. The bare quark spectral density, from Eqs. (3.13) and (3.14), is given by

$$\rho_F(p) = e^{-\mathbf{p}_{\perp}^2/|q_f e B|} (\not{p}_{\parallel} + m_q) \mathcal{P}_{-} \frac{2\pi}{p^0} \left[\delta(p^0 - \varepsilon_{p_z}) + \delta(p^0 + \varepsilon_{p_z}) \right], \quad (3.16)$$

where the dispersion relation for the LLL states, $\varepsilon_{p_z} = \sqrt{p_z^2 + m_q^2}$, is purely two dimensional and is independent of q_f .

Figure 2 shows two diagrams contributing to Eq. (3.12) in the real-time ra-basis, which yields

$$\langle J_r^{\mu}(Q) J_a^{\nu}(-Q) \rangle = - \int \frac{d^4 p}{(2\pi)^4} \text{tr} \left[\gamma^{\nu} S_{ar}(p) \gamma^{\mu} S_{rr}(p+Q) + \gamma^{\nu} S_{rr}(p) \gamma^{\mu} S_{ra}(p+Q) \right]. \quad (3.17)$$

The first thing to notice is that the integration with respect to \mathbf{p}_{\perp} is trivially factorized as

$$4 \int \frac{d^2 \mathbf{p}_{\perp}}{(2\pi)^2} e^{-\mathbf{p}_{\perp}^2/|q_f e B|} e^{-(\mathbf{p}_{\perp} + \mathbf{q}_{\perp})^2/|q_f e B|} = \frac{|q_f e B|}{2\pi} e^{-\mathbf{q}_{\perp}^2/(2|q_f e B|)}. \quad (3.18)$$

This is naturally expected since the transverse dynamics decouples from the longitudinal dynamics of the LLL states; the operator \mathcal{P}_{-} projects the (3+1)-dimensional (Dirac) fermions onto (1+1)-dimensional ones. The factor of $|q_f e B|/(2\pi)$ can be understood as

the transverse density of states for the LLL states. Moreover, from the fact that the transverse γ -matrices (namely, γ^x and γ^y collectively denoted by γ^\perp) satisfy

$$\mathcal{P}_\pm \gamma^\perp = \gamma^\perp \mathcal{P}_\mp, \quad (3.19)$$

we see that the transverse components of the self-energy are zero, i.e. $\Pi_R^{\perp\mu} = \Pi_R^{\mu\perp} = 0$. This is physically clear from the absence of transverse currents with the LLL states. The remaining longitudinal part of the self-energy after performing the integral over (p^0, p_z) in (3.17) should be equivalent to the corresponding one for (1+1)-dimensional Dirac fermion at finite temperature.

We thus have, after summing over quark flavors f ,

$$\Pi_{R,\text{LLL}}^{\mu\nu}(Q) = \pi s(\mathbf{q}_\perp) \Pi_{R,2\text{D}}^{\mu\nu}(\omega, q_z), \quad s(\mathbf{q}_\perp) \equiv 4\alpha_s T_R \sum_f \left(\frac{|q_f e B|}{2\pi} \right) e^{-\frac{q_\perp^2}{2|q_f e B|}}, \quad (3.20)$$

where $\Pi_{R,2\text{D}}^{\mu\nu}(\omega, q_z)$ is the retarded self energy tensor in 1 + 1 dimensions which is dimensionless and is independent of $q_f B$. The gauge-invariance completely fixes its form as $\Pi_{R,2\text{D}}^{\mu\nu}(\omega, q_z) \propto (q_\parallel^2 g_\parallel^{\mu\nu} - q_\parallel^\mu q_\parallel^\nu)$, so that one can write $\Pi_{R,\text{LLL}}^{\mu\nu}$ as

$$\Pi_{R,\text{LLL}}^{\mu\nu}(\omega, \mathbf{q}) \equiv \bar{\Pi}_{\text{LLL}}(\omega, \mathbf{q}) (q_\parallel^2 g_\parallel^{\mu\nu} - q_\parallel^\mu q_\parallel^\nu), \quad (3.21)$$

which defines $\bar{\Pi}_{\text{LLL}}(\omega, \mathbf{q})$. Note that this is the unique gauge-invariant tensor structure in (1+1) dimensions, independently of whether (1+1)-dimensional Lorentz symmetry is broken or not at finite temperature.

From Eq. (3.20) we see that the self-energy from the LLL states is of the order of $\alpha_s e B$. On the other hand, the contributions from hard thermal gluons to the self-energy, for example to the screening mass m_D^2 , is of order $\alpha_s T^2$, which is sub-dominant compared to the LLL contribution by $e B \gg T^2$. We can therefore neglect thermal gluon contributions to the self-energy up to this order. This defines our LO computation in the regime of our interests, $\alpha_s e B \ll T^2 \ll e B$. In section 4 we will find, however, that the longitudinal momentum diffusion coefficient κ_\parallel vanishes in this LO approximation in the massless limit (see the next section for more details), which necessitates including the imaginary part of the thermal gluon contribution to the self-energy to find a non-zero contribution to κ_\parallel . Then, in this way, we can get a first leading non-zero value of κ_\parallel in the $m_q = 0$ limit, which is suppressed by a power of $T^2/(e B)$ as compared to κ_\perp as elucidated in section 5.2. Thus, our definition of “LO” for κ_\parallel in the $m_q = 0$ case should be understood in this sense. We emphasize that our computation for κ_\parallel in the massless limit at this modified LO is also systematic and well-defined in accord with $\alpha_s e B \ll T^2 \ll e B$, as will be explained in section 5.2.

3.2 Scattering rate from the spectral density

Based on the above discussion, let us temporarily neglect thermal gluon contributions to the self-energy for the moment, and the tensor structure of the gluon self energy from the LLL states is then given in Eq. (3.21). We shall first elaborate the tensor structure of the resulting gluon two-point correlation function with the above self-energy.

In general the expression for the A^0 gluon propagator, G_R^{00} , depends on the gauge choice. Nevertheless, the final expression for the Coulomb scattering rate of a static heavy quark is physical and is gauge invariant. A simple way to see the gauge invariance is to note that the gauge transformation of A^0 is of a form, $A^0 \rightarrow A^0 + \omega\alpha$, and since $\langle A^0 \rangle = 0$, the correction to G_R^{00} is of order ω^2 , which vanishes in Eq.(2.9) for the scattering rate in $\omega \rightarrow 0$. We will demonstrate the gauge invariance with two choices of gauge fixing; the covariant and the Coulomb gauges. Inserting the self-energy (3.21), we can write down the general form of the gluon retarded propagator in the covariant gauge as [49]

$$G_R^{00}(Q) = \frac{\omega^2}{Q_\epsilon^4} \left(\frac{\mathbf{q}_\perp^2}{q_\parallel^2} - \xi \right) + \frac{q_z^2}{q_\parallel^2} \left[\frac{1}{Q^2 - q_\parallel^2 \bar{\Pi}_{LLL}(\omega + i\epsilon, \mathbf{q})} \right], \quad (3.22)$$

where $Q_\epsilon^2 \equiv (\omega + i\epsilon)^2 - \mathbf{q}^2$ and ξ is a gauge parameter. Note that we do not insert $i\epsilon$ in Q^2 and q_\parallel^2 that appear in the above, especially in the second part, since they come from the tensor structure in Eq. (3.21) and an $i\epsilon$ in $\bar{\Pi}_{LLL}$ is sufficient to keep the imaginary part correctly. On the other hand, in the Coulomb gauge we have,

$$G_R^{00}(Q) = \frac{1}{\mathbf{q}^2} \frac{1}{Q^2 - q_\parallel^2 \bar{\Pi}_{LLL}(\omega + i\epsilon, \mathbf{q})} \left[Q^2 + \frac{(Q^2 - q_\parallel^2) \omega^2 \bar{\Pi}_{LLL}(\omega + i\epsilon, \mathbf{q})}{\mathbf{q}^2} \right] - \xi \frac{\omega^2}{|\mathbf{q}|^4}. \quad (3.23)$$

We can readily confirm that the above two expressions give an identical form for the scattering rate in the $\omega \rightarrow 0$ limit, i.e.

$$\frac{d\Gamma(\mathbf{q})}{d^3\mathbf{q}} = \frac{4\pi\alpha_s}{(2\pi)^3} C_R^{\text{HQ}} \lim_{\omega \rightarrow 0} \frac{T}{\omega} (-2) \text{Im}[G_R^{00}(\omega, \mathbf{q})] = \frac{\alpha_s T}{\pi^2} C_R^{\text{HQ}} \frac{f_{\text{LLL}}(\mathbf{q})}{[\mathbf{q}^2 + \text{Re} \Pi_{R,LLL}^{00}(\omega = 0, \mathbf{q})]^2}, \quad (3.24)$$

where we introduced $\text{Im} \Pi_{R,LLL}^{00}(\omega, \mathbf{q}) = \omega f_{\text{LLL}}(\mathbf{q})$ for small ω as it is an odd function of ω in general, and we have used Eq. (3.21) to find $\Pi_{R,LLL}^{00}(0, \mathbf{q}) = -q_z^2 \bar{\Pi}_{LLL}(0, \mathbf{q})$.

Before moving to the computation of $\Pi_{R,LLL}^{00}(Q)$ which will be addressed in the next subsection, it would be instructive to recall the well-known picture of heavy quark scatterings (without a strong magnetic field), and compare it with our case of the LLL states. Without magnetic field, the imaginary part of $G_{R,B=0}^{00}$ comes from the imaginary part

of $\Pi_{R,B=0}^{00}$ in the covariant gauge (which is an odd function of ω) or more precisely expressed as $F(Q) \equiv (-Q^2/\mathbf{q}^2)\Pi_{R,B=0}^{00}$ in the common convention of Ref. [52]. As discussed shortly, from the HTL contribution to $\Pi_{R,B=0}^{00}$ for soft Q (i.e. from hard thermal gluons and quarks), the resulting spectral density $\rho_{L,B=0}(Q) = -2\text{Im}[G_{R,B=0}^{00}(Q)]$ receives the following two contributions: (i) The plasmon pole located in a time-like region ($|\omega| > |\mathbf{q}|$). (ii) The continuous part along the space-like interval ($|\omega| < |\mathbf{q}|$) originating from the Landau damping.

The plasmon pole remains gapped even in the $|\mathbf{q}| \rightarrow 0$ limit by the plasma frequency, $\omega^2 \rightarrow m_{\text{pl}}^2 = m_{D,B=0}^2/3$, with the Debye mass $m_{D,B=0}^2 \equiv \text{Re}\Pi_{R,B=0}^{00}(\omega = 0) = (4\pi\alpha_s/3)(N_c + T_R N_f)T^2$. Thus, in our limit of $\omega \rightarrow 0$, the plasmon pole (i) decouples and only the continuous Landau damping part (ii) is relevant. In this case, we can smoothly take the $\omega \rightarrow 0$ limit for $\rho_L(Q)/\omega$, that is,

$$\lim_{\omega \rightarrow 0} (-2) \frac{\text{Im}[G_{R,B=0}^{00}(Q)]}{\omega} = \lim_{\omega \rightarrow 0} \frac{2}{\omega} \frac{\text{Im}\Pi_{R,B=0}^{00}(Q)}{[Q^2 - \text{Re}\Pi_{R,B=0}^{00}(Q)]^2 + [\text{Im}\Pi_{R,B=0}^{00}(Q)]^2} = \frac{2f(\mathbf{q})}{(\mathbf{q}^2 + m_{D,B=0}^2)^2}, \quad (3.25)$$

where we can write $\text{Im}\Pi_{R,B=0}^{00}(\omega \sim 0) = \omega f(\mathbf{q})$ because $\text{Im}\Pi_{R,B=0}^{00}(\omega)$ is an odd function of ω [§], and thus we find a finite scattering rate. From the cutting rules, the physics interpretation is clear; $f(\mathbf{q})$ is an integrated spectrum of scattering particles of momentum transfer \mathbf{q} weighted by thermal distributions, while $1/(\mathbf{q}^2 + m_{D,B=0}^2)^2$ is the square of the screened Coulomb amplitude.

We find that a similar physics interpretation is also possible for the spectral density from the LLL contributions in (3.24). There exists a time-like plasmon pole determined by

$$Q^2 = q_{\parallel}^2 \text{Re} \bar{\Pi}_{LLL}(\omega, \mathbf{q}) \quad (3.26)$$

with a mass of order $m_{\text{pl}}^2 \sim \alpha_s eB$, and the spectral density from this pole is irrelevant in the $\omega = 0$ limit. In the space-like region (and on the light-cone in the massless limit), especially near $\omega = 0$, we will explicitly show that there exists a finite spectral density coming from the Landau damping with the LLL states. In fact, Eq. (3.24) has the precisely same structure as in Eq. (3.25). As mentioned below Eq. (3.25), the factor $f_{\text{LLL}}(\mathbf{q})$ from the imaginary part again represents the integrated spectrum of the scatterers, namely the quarks thermally populated in the LLL states. On the other hand, the real part in

[§]More explicitly, we have $f(\mathbf{q}) = \pi m_D^2/2|\mathbf{q}|$ for soft $\mathbf{q}^2 \sim \alpha_s T^2$, while for ultra hard $|\mathbf{q}| \gg T$, it is Boltzmann suppressed by $f(\mathbf{q}) \sim e^{-|\mathbf{q}|/T}$. Also, it can be shown that $\text{Re}[\Pi_{R,B=0}^{00}(\omega = 0, \mathbf{q})]$ behaves as $\sim \alpha_s T^4/\mathbf{q}^2$ for ultra hard $|\mathbf{q}|$.

the denominator of Eq. (3.24) provides a screening for the Coulomb scattering with the screening mass, $m_{D,B}^2 \sim \alpha_s eB$. We will find that the LO contributions to κ_\perp come from the momentum transfer region $\sqrt{\alpha_s eB} \lesssim |\mathbf{q}_\perp| \lesssim \sqrt{eB}$ as we mentioned below Eq. (2.4). The upper cutoff, \sqrt{eB} , arises from the Gaussian factor of the quark propagator, and it reflects the fact that the LLL states carry intrinsic transverse momentum of order $\sim \sqrt{eB}$ even at $T = 0$ due to their transverse size $l \sim 1/\sqrt{eB}$, and the transverse momentum transfer is bounded not by thermal distribution of the scattering LLL particles (for which the energy levels are independent of q_\perp) but by \sqrt{eB} . This explains why the upper cutoff is not given by T from the Boltzmann factor $e^{-|q|/T}$, which would normally be the case in other finite- T calculations.

4 Massless limit

In this section we consider the case where the light quarks (of representation R) in the LLL states are massless, i.e. $m_q = 0$. We will find some special features originating from the nature of chiral fermions. To evaluate the spectral density in Eq. (3.24), we need to determine $\Pi_{R,\text{LLL}}^{00}$ which, according to Eq. (3.20), is cast into the problem of computing $\Pi_{R,2\text{D}}^{\mu\nu}(\omega, q_z)$ from the massless fermion one-loop in 2D. In this case we can use a powerful technique of bosonization that maps (1+1)-dimensional massless fermions into bosons [53]. The mapping rule is well established as (see for example Ref. [54] and also Ref. [55] for the application to QCD in strong magnetic field)

$$J_{2\text{D}}^\mu = \sqrt{\frac{1}{\pi}} \epsilon^{\mu\nu} \partial_\nu \phi, \quad J_{2\text{D}}^{A,\mu} = \sqrt{\frac{1}{\pi}} \partial_\mu \phi, \quad (4.27)$$

between the vector (axial) current $J_{2\text{D}}^\mu$ ($J_{2\text{D}}^{A,\mu}$) and a real scalar field ϕ . We note that

$$\langle \phi_r(q_\parallel) \phi_a(-q_\parallel) \rangle = \frac{i}{(\omega + i\epsilon)^2 - q_z^2} \quad (4.28)$$

for any temperature T and chemical potential μ , since the retarded two point function of a free theory is independent of (T, μ) . Using this correspondence, we can easily get the retarded current-current correlator in (1+1) dimensions as

$$\begin{aligned} \Pi_{R,2\text{D}}^{\mu\nu}(\omega, q_z) &\equiv i \langle J_r^\mu(q_\parallel) J_a^\nu(-q_\parallel) \rangle_{2\text{D}} = \frac{i \epsilon^{\mu\alpha} \epsilon^{\nu\beta} q_{\parallel\alpha} q_{\parallel\beta}}{\pi} \langle \phi_r(q_\parallel) \phi_a(-q_\parallel) \rangle \\ &= \frac{1}{\pi [(\omega + i\epsilon)^2 - q_z^2]} \left(q_\parallel^2 g_{\parallel}^{\mu\nu} - q_\parallel^\mu q_\parallel^\nu \right). \end{aligned} \quad (4.29)$$

We have explicitly checked the cancelation of all T dependent terms in a direct computation of the fermion loop in Eq. (3.17) at finite T . Consequently, comparing Eqs. (3.20) and (3.21) with Eq. (4.29), we find

$$\text{Re } \Pi_{R,\text{LLL}}^{00}(\omega, \mathbf{q}) = -s(\mathbf{q}_\perp) \frac{q_z^2}{q_\parallel^2}, \quad (4.30a)$$

$$\text{Im } \Pi_{R,\text{LLL}}^{00}(\omega, \mathbf{q}) = \frac{\pi}{2} s(\mathbf{q}_\perp) \omega [\delta(\omega - q_z) + \delta(\omega + q_z)]. \quad (4.30b)$$

As we discussed previously, the spectral density inferred from the imaginary part of $G_R^{00}(Q)$ has two pieces; a plasmon pole and a continuous part from the Landau damping[¶]. It is easy to find that Eq. (3.26) gives rise to a time-like plasmon with the following dispersion relation,

$$\omega^2 = \mathbf{q}^2 + s(\mathbf{q}_\perp) = \mathbf{q}^2 + 4\alpha_s T_R \sum_f \left(\frac{|q_f e B|}{2\pi} \right) e^{-\frac{\mathbf{q}_\perp^2}{2|q_f e B|}}, \quad (4.31)$$

where we have used the real part shown in Eq. (4.30). This is nothing but a plasmon carrying a mass of order of $m_{\text{pl}}^2 \sim \alpha_s e B$ for $\mathbf{q}_\perp^2 \lesssim e B$. This plasmon mass, that exists even in the $m_q = 0$ limit, can be interpreted as a result of Schwinger's anomalous mass generation in (1+1)-dimensional massless gauge theory [57], which is in the present case extended to a theory in (3+1) dimensions with the overall transverse Landau degeneracy factor. It is clear that this time-like plasmon is gapped and it produces no contribution to the static spectral density.

Now, a finite contribution to the Coulomb scattering is obtained by inserting Eq. (4.30) into Eq. (3.24) as

$$\frac{d\Gamma(\mathbf{q})}{d^3\mathbf{q}} = \frac{\alpha_s T}{\pi} C_R^{HQ} \frac{s(\mathbf{q}_\perp)}{[\mathbf{q}^2 + s(\mathbf{q}_\perp)]^2} \delta(q_z), \quad (4.32)$$

where the static limit $\omega \rightarrow 0$ in Eq. (4.30) results in the delta function of $q_z \rightarrow 0^\pm$, and we repeat the definition of $s(\mathbf{q}_\perp)$

$$s(\mathbf{q}_\perp) = 4\alpha_s T_R \sum_f \left(\frac{|q_f e B|}{2\pi} \right) e^{-\frac{\mathbf{q}_\perp^2}{2|q_f e B|}}. \quad (4.33)$$

[¶]There is a $Q^2 = 0$ pole in the covariant gauge that does not exist in the Coulomb gauge, and one may wonder how they can be consistent. This difference is well-known. As explained in Ref. [56], the Coulomb gauge has two polarizations corresponding to the physical modes, while the covariant gauge has extra two unphysical modes. Those additional degrees of freedom give rise to $Q^2 = 0$ pole in such a way not to affect physical observables, and so we can discard this pole safely.

This is a central result in this section. One can easily compute the leading order heavy quark damping rate from this.

This delta function $\delta(q_z)$ associated with the LLL states can be understood from a simple kinematic constraint with (1+1)-dimensional massless fermions. These fermions have dispersion relations, $E(p) = \pm p_z$, where the sign refers to the chirality. Since perturbative QCD interactions do not flip the chirality, the energy-momentum transfer from these massless fermions, $(\Delta E, \Delta p_z) = (\omega, q_z)$, must satisfy $\omega = \pm q_z$. Then, the static limit $\omega \rightarrow 0$ imposes the vanishing longitudinal momentum transfer, which is represented by the delta function $\delta(q_z)$.

First, we immediately conclude from Eqs. (2.8) and (4.32) that the longitudinal momentum diffusion coefficient from the LLL states is strictly zero because of the vanishing longitudinal momentum transfer constrained by the kinematics in the massless case at LO. In contrast to this, as we will see in section 5.1, a finite light quark mass introduces $\kappa_{\parallel} \propto m_q^2 \neq 0$ at LO. We will also see in section 5.2 that κ_{\parallel} acquires a non-zero contribution from the scatterings with the hard thermal gluons (but the exchanged gluon is still screened by the LLL states at LO). The resulting κ_{\parallel} is smaller than κ_{\perp} by a factor of T^2/eB .

From the above leading order scattering rate, we can finally obtain the transverse momentum diffusion coefficient as

$$\kappa_{\perp} = \frac{\alpha_s T}{2\pi} C_R^{\text{HQ}} \int d^2 q_{\perp} |\mathbf{q}_{\perp}|^2 \frac{s(\mathbf{q}_{\perp})}{[|\mathbf{q}_{\perp}|^2 + s(\mathbf{q}_{\perp})]^2} = 2\alpha_s^2 T C_R^{\text{HQ}} T_R \left(\frac{eB}{2\pi} \right) K(a), \quad (4.34)$$

where we defined an integral as

$$K(a) = \int_0^{\infty} dx \frac{x \sum_f |q_f| e^{-x/|q_f|}}{[x + a \sum_f |q_f| e^{-x/|q_f|}]^2}, \quad (4.35)$$

with dimensionless variables $x \equiv |\mathbf{q}_{\perp}|^2/2eB$ and $a \equiv \alpha_s T_R/\pi$. It is easy to see that the leading log contribution in α_s comes from the range $\alpha_s \lesssim x \lesssim 1$ or equivalently $\sqrt{\alpha_s eB} \lesssim |\mathbf{q}_{\perp}| \lesssim \sqrt{eB}$ as pointed out before. In this range, the integrand is approximately $1/x$, and the integration produces the leading log behavior as $\sim \log(1/\alpha_s)$. A more careful evaluation gives the full LO result including the constant under the logarithm as

$$\kappa_{\perp}^{\text{LO}} = 2\alpha_s^2 T C_R^{\text{HQ}} T_R \left(\frac{eB}{2\pi} \right) \cdot Q_{\text{em}} \left[\log\left(\frac{1}{\alpha_s}\right) - \log\left(\frac{T_R}{\pi}\right) - \gamma_E - 1 + \sum_f \frac{|q_f|}{Q_{\text{em}}} \log\left(\frac{|q_f|}{Q_{\text{em}}}\right) \right], \quad (4.36)$$

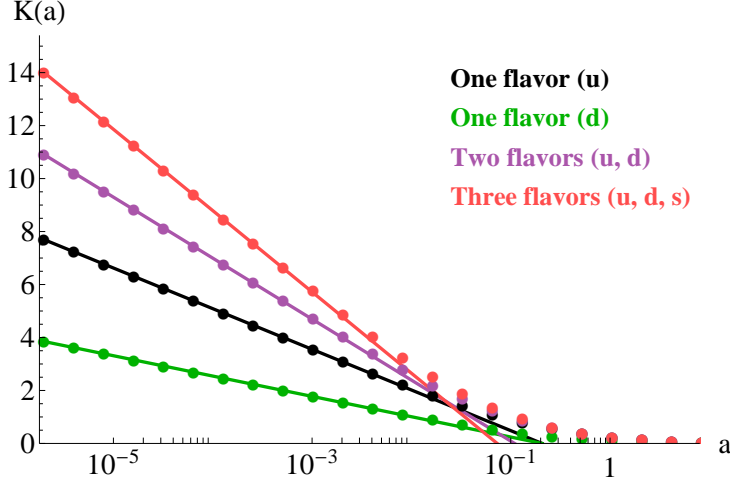


Figure 3: Integral (4.35) for the transverse momentum diffusion coefficient. Lines show the analytic expressions given in between the brackets in Eqs. (4.36), which are confirmed by the numerical integration shown by filled circles.

where $\gamma_E \approx 0.577$ is the Euler-Mascheroni constant, and the sum of electric charges is defined by $Q_{\text{em}} = \sum_f |q_f|$. As shown in Fig. 3, we have numerically checked that this final form is a good approximation to Eq. (4.34) as long as $a \sim \alpha_s \ll 1$.

Let us briefly discuss contributions of the higher Landau levels (hLLs) which are suppressed both in the vacuum and the thermal parts of the gluon self-energy in the strong B limit. First, we should note that the momentum transfer q corresponds to the external momentum of the gluon self-energy and that only the space-like momentum transfer ($q_{\parallel}^2 - q_z^2 < 0$) contributes to the heavy quark momentum diffusion. In the vacuum part, contributions from the hLLs are suppressed because quarks and antiquarks have the dispersion relation, $p_{\parallel}^2 = m_q^2 + 2neB$ ($n \geq 1$), and the off-shellness is of order of eB , which is because the momentum q_{\parallel}^2 is located away from the pair creation threshold (i.e. on-shell point) by eB [49]. Therefore, one can conclude that contributions from the hLLs are suppressed at least by $\mathcal{O}(1/eB)$ when either a quark or an antiquark is excited to a hLL, and by $\mathcal{O}(1/eB^2)$ when both of them belong to hLLs. As for the thermal part, contributions from the hLL are exponentially suppressed by the Boltzmann factor $\sim e^{-\sqrt{2neB}/T}$.

5 Finite contributions to the longitudinal momentum diffusion coefficient

As we have seen in the previous section, the longitudinal momentum diffusion coefficient vanishes when we consider only the massless quarks in the LLL states. This is a consequence of the massless (1+1)-dimensional dispersion relation of the LLL states, which does not allow for any longitudinal momentum transfer at $\omega = 0$. In this section, we examine light-quark mass corrections and thermal gluon contributions.

5.1 Light-quark mass effects

In this subsection we consider finite mass corrections to κ_{\parallel} , which can relax the constraint of the longitudinal momentum transfer that is strictly prohibited in the massless case. First we emphasize that the basic structure of the gluon self-energy shown in Eqs. (3.20) and (3.21) are still valid regardless of the quark mass. Then, one will immediately find that the expression of the spectral density (3.24) is also intact and that the problem reduces to computation of $\Pi_{R,2D}^{\mu\nu}(\omega, q_z)$ that should replace the massless (4.29) with the massive one.

We should notice that the transverse dynamics of LLL quarks are not directly affected by mass corrections as clearly seen in the propagators (3.13)–(3.15). Therefore, the gluon self-energy can be written in the same form as Eq. (3.20):

$$\Pi_R^{\mu\nu}(\omega, q_z) = \pi s(\mathbf{q}_{\perp}) \Pi_{R,2D}(\omega, q_z) (q_{\parallel}^2 g_{\parallel}^{\mu\nu} - q_{\parallel}^{\mu} q_{\parallel}^{\nu}), \quad (5.37)$$

$$\Pi_{R,2D}(\omega, q_z) = \Pi_{R,2D}^{\text{vac}}(q_{\parallel}^2) + \Pi_{R,2D}^{\text{th}}(\omega, q_z). \quad (5.38)$$

This is due to the fact that there is only one gauge-invariant tensor structure in (1+1) dimensions, so that the tensor structure in Eq. (3.21) also persists without modification at finite T . Since we have an overall factor of eB , the coefficient functions, $\Pi_{R,2D}^{\text{vac}}(q_{\parallel}^2)$ and $\Pi_{R,2D}^{\text{th}}(\omega, q_z)$, are dimensionless. We note that, while $\Pi_{R,2D}^{\text{vac}}(q_{\parallel}^2)$ depends on q_{\parallel}^2 in a boost invariant manner, $\Pi_{R,2D}^{\text{th}}(\omega, q_z)$ depends on ω and q_z separately due to finite temperature effects.

First, let us consider the vacuum part. The vacuum part has been explicitly computed

previously in Refs. [49, 51, 58] and takes the following form

$$\Pi_{R,2D}^{\text{vac}}(q_{\parallel}^2) = \frac{1}{\pi[(\omega + i\epsilon)^2 - q_z^2]} \left[1 - \frac{(2m_q)^2}{\sqrt{q_{\parallel}^2[(2m_q)^2 - q_{\parallel}^2]}} \arctan\left(\frac{q_{\parallel}^2}{\sqrt{q_{\parallel}^2[(2m_q)^2 - q_{\parallel}^2]}}\right) \right], \quad (5.39)$$

for $q_{\parallel}^2 \leq 0$. We can deduce an expression for $q_{\parallel}^2 > 0$ using the analytic continuation. The first term corresponds to the massless Schwinger model as discussed in section 4, and the mass correction has an overall factor of m_q^2 . Therefore, as expected from the dimensional argument, the mass correction comes with a function of the dimensionless ratio m_q^2/q_{\parallel}^2 . We will shortly see that the leading order result comes from the momentum transfer range $|\mathbf{q}|^2 \sim m_{D,B}^2 \sim \alpha_s eB$, so that $m_q^2/q_{\parallel}^2 \sim m_q^2/(\alpha_s eB)$. In realistic situations, the light quark mass, $m_q \sim 5 \text{ MeV}$, is much smaller than other scales, so that we will explore a specific regime, $m_q^2 \ll \alpha_s eB$, and compute the longitudinal momentum diffusion coefficient $\kappa_{\parallel}^{\text{LO, massive}}$ to the first non-vanishing order in terms of $m_q^2/(\alpha_s eB)$. Within this hierarchy, we can safely neglect the $m_q \neq 0$ correction to the real part of the self-energy, that is $m_{D,B}^2$, which is of order $m_q^2/(\alpha_s eB)$ smaller compared to the massless case.

In contrast to the massless case, $\Pi_{R,2D}^{\text{vac}}(q_{\parallel}^2)$ acquires an imaginary part above the threshold of the pair creation at $q_{\parallel}^2 = (2m_q)^2 > 0$. However, this imaginary part in the time-like region does not contribute to the heavy quark momentum diffusion in the static limit.

We next compute the thermal part starting with Eq. (3.17), which can be finally cast into the following form (introducing a compact notation $Q = (\omega, q_z)$),

$$\Pi_{R,2D}^{\text{th}}(Q) = \frac{m_q^2}{q_{\parallel}^2} \left[J_0(Q) + 2 \frac{q_z}{q_{\parallel}^2} J_1(Q) \right], \quad (5.40)$$

with the definition

$$J_{\beta}(Q) \equiv \int_{-\infty}^{\infty} \frac{dp_z}{2\pi} \left[\frac{n_+(\varepsilon_{p_z}) + n_-(\varepsilon_{p_z})}{\varepsilon_{p_z}} \right] \frac{p_z^{\beta}}{(p_z - \frac{1}{2}q_z)^2 - \frac{\omega^2}{4q_{\parallel}^2}[q_{\parallel}^2 - (2m_q)^2] - i\omega\epsilon}, \quad (5.41)$$

where $\beta = 0, 1$ and we introduce $\varepsilon_{p_z} \equiv \sqrt{p_z^2 + m_q^2}$ and $n_{\pm}(\varepsilon_p) \equiv [e^{(\varepsilon_p \mp \mu)/T} + 1]^{-1}$. We simplified the retarded $i\epsilon$ -prescription (i.e. $\omega \rightarrow \omega + i\epsilon$) in Eq. (5.41) for small ω . We note that $\Pi_{R,2D}^{\text{th}}(Q)$ again has an overall factor of m_q^2 as in the vacuum part. Therefore, the mass correction goes like m_q^2/q_z^2 and m_q^2/T^2 and they are negligible for the real part of the self-energy or the screening mass.

The only important effect for us is the mass corrections to the imaginary part of $\Pi_{R,2D}^{\text{th}}(Q)$, which appear from the singularities in the integral at $\omega^2 = 0$ and $\omega = (2m_q)^2$.

The imaginary part appearing from the factor of $1/q_{\parallel}^2$ is again the contribution of the forward scattering as in the massless case, so that it does not contribute to the longitudinal momentum diffusion. It is instructive to see another expression which can be obtained by taking the static limit $\omega \rightarrow 0$ in Eq. (17) of Ref. [59] (in the absence of charge chemical potential) as

$$\lim_{\omega \rightarrow 0} \left[\frac{\text{Im} \Pi_R^{00}(Q)}{\omega} \right] = \frac{1}{2T} \int dk_z \left(1 + \frac{k_z k'_z + m_q^2}{\varepsilon_{k_z} \varepsilon_{k'_z}} \right) n_F(\varepsilon_{k_z}) [1 - n_F(\varepsilon_{k'_z})] \delta(\varepsilon_{k_z} - \varepsilon_{k'_z}), \quad (5.42)$$

where we defined $k'_z = k_z + q_z$. The expression in the curly brackets in Eq. (5.42) agrees with the four-dimensional analogue of Eq. (4) in Ref. [46]. The δ -function in (5.42) can be worked out explicitly as

$$\delta(\varepsilon_{k_z} - \varepsilon_{k'_z}) = \frac{\varepsilon_{q_z/2}}{|q_z|} \delta(k_z + q_z/2), \quad (5.43)$$

which indicates that only a backward scattering $k_z = -k'_z = q_z/2$ contributes to the momentum diffusion of heavy quarks because of the static limit in (1+1) dimensions. We should note again that even such backward scatterings were not allowed for massless quarks as already discussed in Sec. 4.

By performing the k_z integration in Eq. (5.42) or by taking the $\omega \rightarrow 0$ limit in Eq. (5.40), we find

$$\lim_{\omega \rightarrow 0} \left[\frac{\text{Im} \Pi_{R, \text{LLL}}^{00}(Q)}{\omega} \right] = m_q^2 \frac{\pi s(\mathbf{q}_{\perp})}{T |q_z| \varepsilon_{q_z/2}} n_F(\varepsilon_{q_z/2}) [1 - n_F(\varepsilon_{q_z/2})], \quad (5.44)$$

where $s(\mathbf{q}_{\perp})$ is defined in Eq. (3.20). Plugging this into Eq. (3.24) as before, we can obtain the scattering rate $d\Gamma(\mathbf{q})/d^3\mathbf{q}$, and then the finite mass correction to κ_{\parallel} as

$$\kappa_{\parallel}^{\text{LO, massive}} = \frac{\alpha_s}{\pi} C_R^{\text{HQ}} m_q^2 \int d^3\mathbf{q} \frac{s(\mathbf{q}_{\perp})}{[\mathbf{q}^2 + s(\mathbf{q}_{\perp})]^2} \frac{|q_z|}{\varepsilon_{q_z/2}} \frac{1}{1 + \cosh(\varepsilon_{q_z/2}/T)}. \quad (5.45)$$

Now, it is clear from this expression that the dominant contribution indeed comes from a region, $|\mathbf{q}| \sim (\alpha_s e B)^{\frac{1}{2}}$, as claimed before. In this region the Gaussian is approximated as $e^{-\mathbf{q}_{\perp}^2/(2eB)} \sim 1$, and we can replace $s(\mathbf{q}_{\perp})$ by an effective Debye mass in the presence of the magnetic field as

$$m_{D,B}^2 \equiv s(\mathbf{q}_{\perp} = 0) = 4\alpha_s T_R \sum_f \left(\frac{|q_f e B|}{2\pi} \right). \quad (5.46)$$

Furthermore, at the leading order in $m_q^2/\alpha_s e B$, we can approximate the quasi-energy as

$$\varepsilon_{q_z/2} = \sqrt{(q_z/2)^2 + m_q^2} \sim |q_z/2| \quad (5.47)$$

in Eq. (5.45). Since $q_z \sim (\alpha_s e B)^{1/2} \ll T$, we can also make an approximation as $\cosh(\varepsilon_{qz}/2/T) \simeq 1$ in Eq. (5.45). Putting those pieces together, we arrive at

$$\begin{aligned}\kappa_{\parallel}^{\text{LO, massive}} &\simeq \frac{\alpha_s}{2\pi} C_R^{\text{HQ}} m_q^2 \int d^3 \mathbf{q} \frac{m_{D,B}^2}{(\mathbf{q}^2 + m_{D,B}^2)^2} \\ &= \frac{\pi}{2} \alpha_s C_R^{\text{HQ}} m_q^2 m_{D,B} = \frac{1}{2} \alpha_s C_R^{\text{HQ}} m_q^2 \sqrt{\alpha_s e B} \sqrt{2\pi T_R Q_{\text{em}}}. \quad (5.48)\end{aligned}$$

We should note that this result is independent of T after dropping terms in our assumed regime: $m_q^2 \ll \alpha_s e B \ll T^2 \ll e B$. Thus, if m_q or $q_z \sim (\alpha_s e B)^{1/2}$ were comparable to T , the mass correction would be a T dependent function of m_q/T and $(\alpha_s e B)^{1/2}/T$, which are all dropped systematically in our approximation.

5.2 Thermal gluon contributions

We can capture the scatterings with thermal gluons by including the imaginary part of the self-energy, $\Pi_{R, \text{gluon}}^{00}$, coming from hard thermal gluons. A quick power counting shows that it is enough to keep only the imaginary part of $\Pi_{R, \text{gluon}}^{00}$, not the real part, for a first non-vanishing contribution to κ_{\parallel} , which we will refer to as “leading order” and will denote by $\kappa_{\parallel}^{\text{LO, gluon}}$. The real part will be a sub-leading correction to the leading-order screening mass from the quark loop $m_{D,B}^2 \sim \alpha_s e B$, and we can neglect the gluon contribution in our regime. We will find that the final result of $\kappa_{\parallel}^{\text{LO, gluon}}$ is relatively suppressed by $T^2/(eB)$ compared to $\kappa_{\perp}^{\text{LO}}$ obtained in the preceding subsection. Consequently, to leading order we can replace Eq. (3.25) with

$$\lim_{\omega \rightarrow 0} (-2) \text{Im} \left[\frac{G_{R, \text{gluon}}^{00}(Q)}{\omega} \right] = \lim_{\omega \rightarrow 0} \frac{2}{\omega} \frac{\text{Im} \Pi_{R, \text{gluon}}^{00}(Q)}{[Q^2 - \text{Re} \Pi_{R, \text{LLL}}^{00}(Q)]^2}, \quad (5.49)$$

neglecting the thermal gluon contribution to the screening mass as compared to $\Pi_{R, \text{LLL}}^{00}(Q)$ from the LLL quarks.

The dominant contribution to the imaginary part of the self-energy comes from thermal gluons with hard momenta $\sim T$, which is understood based on the interplay between phase space volume and the Boltzmann suppression. The dispersion relation of these hard gluons could get modified in general by thermal effects. Since $\alpha_s e B \gg \alpha_s T^2$, however, the main source of the correction appears from LLL quark loops, and in our regime, $T^2 \gg \alpha_s e B$, we should neglect such corrections and treat hard gluons as free quasi-particles.

As a result, the imaginary part, $\text{Im} \Pi_{R, \text{gluon}}^{00}(Q)$ is identical to the one without B , given by a cut of gluon one-loop contribution to $\Pi_{R, \text{gluon}}^{00}$ which is equal to the integrated

spectrum of scattering thermal gluons with Coulomb vertex. Equivalently, we can follow Ref. [39] and work out directly the t -channel scattering rate with thermal gluons with the screened Coulomb propagator given above. In this way the scattering rate reads:

$$(2\pi)^3 2M_Q \frac{d\Gamma_{\text{gluon}}}{d^3\mathbf{q}} = \frac{1}{2M_Q} \int \frac{d^3\mathbf{k}}{(2\pi)^3 2|\mathbf{k}|} \frac{d^3\mathbf{k}'}{(2\pi)^3 2|\mathbf{k}'|} (2\pi)^4 \delta^{(4)}(k' + Q - k) |\mathcal{M}|^2 n_B(|\mathbf{k}|) [1 + n_B(|\mathbf{k}'|)], \quad (5.50)$$

where the t -channel amplitude with incoming and outgoing gluons of color and polarization (b, ϵ^μ) and $(c, \tilde{\epsilon}^\mu)$ is given by

$$\mathcal{M}^{bc} = -i4\pi\alpha_s f^{abc} [\bar{U}(P+Q)\gamma^0 t_R^a U(P)] G_{ra}^{00}(Q)(|\mathbf{k}| + |\mathbf{k}'|)(\epsilon \cdot \tilde{\epsilon}^*), \quad (5.51)$$

where we included only A^0 Coulomb interaction for heavy quarks in the static limit $P = (M_Q, \mathbf{0})$. In this case the heavy quark spinors can simplify as

$$\bar{U}(P+Q)\gamma^0 U(P) \simeq \bar{U}^\dagger(P)U(P) = 2M_Q. \quad (5.52)$$

Color summation in the squared amplitude gives

$$\sum_{a,a',b,c} f^{abc} f^{a'bc} (t_R^a t_R^{a'}) = N_c \sum_a t_R^a t_R^a = N_c C_R^{\text{HQ}} \mathbf{1}, \quad (5.53)$$

and the polarization sum is

$$\sum_{\epsilon, \tilde{\epsilon}} |\epsilon \cdot \tilde{\epsilon}^*|^2 = 1 + \cos^2 \theta_{\mathbf{k}\mathbf{k}'}, \quad (5.54)$$

where $\theta_{\mathbf{k}\mathbf{k}'}$ is the angle between \mathbf{k} and \mathbf{k}' . In the static limit we have $|\mathbf{k}'| = |\mathbf{k}|$ and from this the scattering rate becomes

$$\frac{d\Gamma_{\text{gluon}}}{d^3\mathbf{q}} = 4\alpha_s^2 N_c C_R^{\text{HQ}} \int \frac{d^3\mathbf{k}}{(2\pi)^3} \delta(|\mathbf{k}| - |\mathbf{k} - \mathbf{q}|) |G_{ra}^{00}(Q)|^2 (1 + \cos^2 \theta_{\mathbf{k}\mathbf{k}'}) n_B(|\mathbf{k}|) [1 + n_B(|\mathbf{k}|)]. \quad (5.55)$$

We can carry out the $\theta_{\mathbf{k}\mathbf{k}'}$ -angle integration of \mathbf{k} using $\delta(|\mathbf{k}| - |\mathbf{k} - \mathbf{q}|) = |\mathbf{q}|^{-1} \delta[\cos \theta_{\mathbf{k}\mathbf{q}} - |\mathbf{q}|/(2|\mathbf{k}|)] \Theta(|\mathbf{k}| - |\mathbf{q}|/2)$ and $\cos \theta_{\mathbf{k}\mathbf{k}'} = 1 - |\mathbf{q}|^2/(2|\mathbf{k}|^2)$, and after all we obtain

$$\frac{d\Gamma_{\text{gluon}}}{d^3\mathbf{q}} = \frac{\alpha_s^2}{\pi^2} N_c C_R^{\text{HQ}} \frac{|G_{ra}^{00}(Q)|^2}{|\mathbf{q}|} \int_{|\mathbf{q}|/2}^{\infty} dk k^2 \left[1 + \left(1 - \frac{\mathbf{q}^2}{2k^2} \right)^2 \right] n_B(k) [1 + n_B(k)], \quad (5.56)$$

where the screened Coulomb amplitude is

$$|G_{ra}^{00}(Q)|^2 = \frac{1}{[\mathbf{q}^2 + \text{Re} \Pi_{R,\text{LL}}^{00}(Q)]^2}. \quad (5.57)$$

We note that in the computation of κ_{\parallel} rotational asymmetry arises only from $s(\mathbf{q}_{\perp}) = \text{Re } \Pi_{R,\text{LLL}}^{00}(\omega = 0, \mathbf{q})$ as defined in Eq. (4.30).

The Boltzmann suppression in $d\Gamma/d^3\mathbf{q}$ restricts $k \lesssim T$, and this in turn gives $|\mathbf{q}| \lesssim T$ from the integration boundary. Since $T^2 \ll eB$, the asymmetric factor $e^{-q_{\perp}^2/(2eB)}$ in $s(\mathbf{q}_{\perp})$ is nearly the unity up to corrections in powers of $T^2/(eB)$. Therefore, at LO we recover rotational symmetry that allows us to replace $(q_z)^2$ with $q^2/3 \equiv |\mathbf{q}|^2/3$, and we arrive at

$$\kappa_{\parallel}^{\text{LO, gluon}} = \frac{4\alpha_s^2}{3\pi} N_c C_R^{\text{HQ}} \int_0^\infty dq \frac{q^3}{(q^2 + m_{D,B}^2)^2} \int_{q/2}^\infty dk k^2 \left[1 + \left(1 - \frac{q^2}{2k^2} \right)^2 \right] n_B(k) [1 + n_B(k)]. \quad (5.58)$$

Apart from the value of the Debye mass $m_{D,B}^2$ defined in Eq. (5.46), this integral is apparently identical to the conventional one without B shown in Ref. [39, 46]. Therefore, the result of the integral can be obtained by simply substituting our $m_{D,B}$ for the conventional Debye mass in Refs. [39, 46] as

$$\kappa_{\parallel}^{\text{LO, gluon}} = \frac{4\pi\alpha_s^2}{9} N_c C_R^{\text{HQ}} T^3 \left[\log\left(\frac{1}{\alpha_s}\right) - \log\left(\frac{T_R Q_{\text{em}} eB}{2\pi T^2}\right) + 2\xi \right], \quad (5.59)$$

where $\xi = \frac{1}{2} - \gamma_E + \frac{\zeta'(2)}{\zeta(2)} \simeq -0.64718$. This result is $T^2/(eB)$ smaller than $\kappa_{\perp}^{\text{LO}}$ in Eq. (4.36).

The above evaluation is systematic and consistent with our basic assumption $\alpha_s eB \ll T^2 \ll eB$. First, as discussed in the beginning of this section, we neglected the thermal gluon contribution to the Debye mass $\sim gT \ll m_{D,B}$. Next, in Ref. [39, 46], the authors obtained the LO result from the contributions of the hard thermal gluons $\gtrsim T$, and neglected corrections of the order of $m_D^2/T^2 \sim g^2$ from the contributions of the soft gluons $\sim m_D$. In our case, we can also neglect these corrections $\sim m_{D,B}^2/T^2 \sim \alpha_s eB/T^2 \ll 1$ along with the above hierarchy in the present analysis at the LO accuracy. We leave studies of the higher-order contributions for the future work, which also have relevance to the QCD Kondo effect recently discussed in Refs. [60, 61].

It is instructive to compare the LO hard thermal gluon contribution (5.59) with the LO massive light quark contribution to κ_{\parallel} in Eq. (5.48). The ratio is found to be,

$$\frac{\kappa_{\parallel}^{\text{LO, massive}}}{\kappa_{\parallel}^{\text{LO, gluon}}} \sim \frac{\alpha_s (\alpha_s eB)^{1/2} m_q^2}{\alpha_s^2 T^3} = \left(\frac{m_q^2}{\alpha_s eB} \right) \left(\frac{\alpha_s eB}{T^2} \right)^{1/2} \left(\frac{eB}{T^2} \right). \quad (5.60)$$

The first two factors are small according to our working regime, but the last factor can be large. Therefore, the massive contribution $\kappa_{\parallel}^{\text{LO, massive}}$ could be in principle as comparably large as $\kappa_{\parallel}^{\text{LO, gluon}}$, and this happens when $eB \sim \alpha_s (T^6/m_q^4)$. Then, to be consistent with

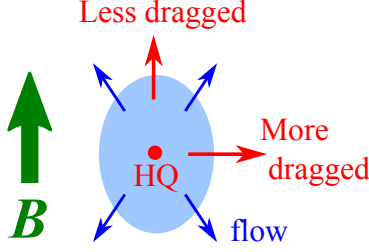


Figure 4: Schematic illustration for the mechanism to derive an additional contribution to the elliptic flow of heavy quarks. Because of $\kappa_{\perp} \gg \kappa_{\parallel}$ heavy quarks are more dragged along the in-plane than along the out-of-plane.

our assumed regime, $\alpha_s eB \ll T^2$, we have a constraint of $\alpha_s \ll m_q^2/T^2$, which is not quite likely true in the heavy ion collisions. Hence, in realistic heavy ion experiments, $\kappa_{\parallel}^{\text{LO, gluon}}$ is dominant contribution to the longitudinal diffusion coefficient.

6 Phenomenological implications

In the previous sections, we have computed the heavy quark momentum diffusion coefficients, κ_{\perp} and κ_{\parallel} , in the QGP in the presence of strong magnetic field $eB \gg T^2$ at LO in α_s , and have found

$$\frac{\eta_{\parallel}(B)}{\eta_{\perp}(B)} = \frac{\kappa_{\parallel}(B)}{\kappa_{\perp}(B)} \sim \frac{T^2}{eB} \ll 1. \quad (6.61)$$

We now study the phenomenological implications of Eq. (6.61).

To give a (semi-)quantitative estimate of its influence on the elliptic flow of heavy quarks, we will implement the anisotropic $\kappa_{\perp, \parallel}$ in description of the evolution of an open heavy quark in the expanding QGP (see Fig. 4 for a schematic illustration of our physical picture). Following conventions in the heavy ion collision literature, we will take the in-plane and out-of-plane direction as x - and y -direction, respectively. We will assume an external magnetic field along the y -direction. Therefore, $\kappa_{xx} = \kappa_x = \kappa_{\perp}$ and $\kappa_{yy} = \kappa_y = \kappa_{\parallel}$. In realistic situations in the heavy ion collisions, the background flow $u_{x,y}$ of plasma fireball depends on space and time. In what follows we limit ourselves to some spatial regions where we can treat $u_{x,y}$ as spatially homogeneous fields.

The evolution of a heavy quark is described by the Langevin equation with the homogeneous flow effects (M_Q is the heavy quark mass)

$$\frac{dp_x}{d\tau} = -\eta_x(\tau) \left[p_x - M_Q u_x(\tau) \right] + \xi_x(\tau), \quad \frac{dp_y}{d\tau} = -\eta_y(\tau) \left[p_y - M_Q u_y(\tau) \right] + \xi_y(\tau) \quad (6.62)$$

with

$$\langle \xi_x(\tau) \xi_x(\tau') \rangle = \kappa_x \delta(\tau - \tau'), \quad \langle \xi_y(\tau) \xi_y(\tau') \rangle = \kappa_y \delta(\tau - \tau'). \quad (6.63)$$

Equivalently to Eq. (6.62), we can translate these equations into the Fokker-Planck equation as

$$\begin{aligned} \partial_\tau P(p_x, p_y; \tau) = & - \left[\eta_x(\tau) \partial_{p_x} \{ [p_x - M_Q u_x(\tau)] + [M_Q T(\tau)] \partial_{p_x} \} \right. \\ & \left. + \eta_y(\tau) \partial_{p_y} \{ (p_y - M_Q u_y(\tau)) + (M_Q T(\tau)) \partial_{p_y} \} \right] P(p_x, p_y; \tau), \end{aligned} \quad (6.64)$$

where $P(p_x, p_y; \tau)$ denotes the probability of finding a heavy quark at p_x and p_y , and $T(\tau)$ is the time-dependent temperature of the background plasma.

The Green's function to Eq. (6.64), i.e. the probability of finding a heavy quark in (p_x, p_y) at time τ under the initial condition in (p_x^0, p_y^0) can be found analytically as

$$\langle p_x, p_y | p_x^0, p_y^0 \rangle = \prod_{i=x,y} \frac{1}{\sqrt{2\pi\Delta_i(\tau)}} \exp \left\{ - \frac{[p_i - \bar{p}_i(\tau) - p_i^0 e^{-\Gamma_i(\tau)}]^2}{2\Delta_i(\tau)} \right\}. \quad (6.65)$$

Here we introduced new variables:

$$\Gamma_i(\tau) \equiv \int_{\tau_0}^{\tau} d\tau' \eta_i(\tau'), \quad (6.66)$$

$$\bar{p}_i(\tau) \equiv M_Q e^{-\Gamma_i(\tau)} \int_{\tau_0}^{\tau} d\tau' e^{\Gamma_i(\tau')} \eta_i(\tau') u_i(\tau'), \quad (6.67)$$

$$\Delta_i(\tau) \equiv 2M_Q e^{-2\Gamma_i(\tau)} \int_{\tau_0}^{\tau} d\tau' e^{2\Gamma_i(\tau')} [T(\tau') \eta_i(\tau')]. \quad (6.68)$$

With Eq. (6.65) the solution to Eq. (6.64) under the initial condition $P_0(p_x, p_y; \tau_0)$ can be written as

$$P(p_x, p_y; \tau) = \int dp_x^0 dp_y^0 \langle p_x, p_y | p_x^0, p_y^0 \rangle P_0(p_x^0, p_y^0; \tau_0). \quad (6.69)$$

The physical meaning of each term in Eq. (6.66) is rather transparent: $\Gamma_i(\tau)$ is the effective damping factor which will wash out the memory of earlier distribution of heavy quarks. Indeed, a large value of $\Gamma_i(\tau)$ would suppress p_i^0 dependence in the Green's function. \bar{p}_i is nothing but the solution to the Langevin equation (6.64) with homogenous initial condition $p_i = 0$ after averaging over the noise. It characterizes the heavy quark flow due to dragging by the expanding QGP medium. Finally, $\Delta_i(\tau)$ is generated by the noise during the Langevin dynamics, which would blur the information contained in the initial distribution.

The modified distribution of heavy quarks has a characteristic structure as illustrated in Fig. 5. For low momentum, i.e. $p_T \lesssim |\mathbf{u}|M_Q$, the anisotropy in $\eta_{\perp,||}$ or $\kappa_{\perp,||}$ gives rise

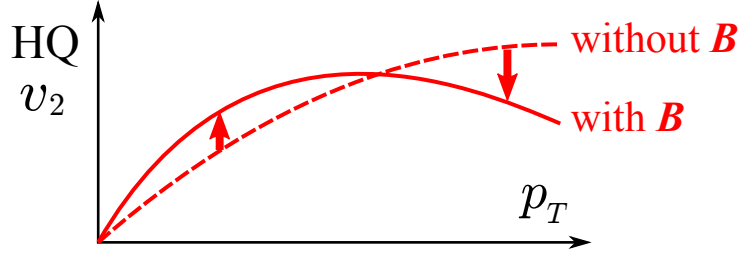


Figure 5: Schematic illustration for the effects of the magnetic field on the heavy quark elliptic flow.

to a positive contribution to v_2 of heavy quarks. This is because, when $\eta_x \gg \eta_y$, heavy quarks will gain more momenta in the x -direction than that in the y -direction, which is embodied in \bar{p}_i terms in Eq. (6.65). In contrast, for high momentum, i.e. $p_T \gtrsim |\mathbf{u}|M_Q$, the magnetically induced contribution to the v_2 is opposite. This is because, for an isotropic initial distribution, more memory is washed out in the x -direction than in the y -direction, which is embodied in $p_i e^{-\Gamma_i}$ terms in Eq. (6.65). More elaborate numerical simulations are under progress.

7 Summary

In this work, we have computed heavy quark momentum diffusion rate κ of a quark-gluon plasma in the presence of strong magnetic fields $eB \gg T^2$ at the leading order in α_s . While the contribution from thermal gluons is still isotropic at the leading order in T^2/eB (c.f. section 5.2), we found that the fermionic contribution becomes anisotropic. Indeed, in the massless limit, the fermionic contribution to the longitudinal diffusion κ_{\parallel} vanishes under the LLL approximation (c.f section 4), while their contributions in the transverse direction shown in Eq. (4.36) is non-vanishing $\kappa_{\perp} \sim \alpha_s^2 eBT$ and is dominant over the gluonic contributions. As a result, we have a large anisotropy

$$\frac{\eta_{\parallel}}{\eta_{\perp}} = \frac{\kappa_{\parallel}}{\kappa_{\perp}} \sim \frac{T^2}{eB} \ll 1. \quad (7.70)$$

We call this anisotropy in the drag force coefficients “magnetic drag anisotropy.”

Turning to the phenomenological implications of “magnetic drag anisotropy”, we first recall that for heavy quarks in an expanding plasma, the drag force will push them to co-move with the medium. For low momentum heavy quarks, the anisotropy $\eta_{\parallel} < \eta_{\perp}$ implies that those heavy quarks will gain more momentum in the in-plane direction than in the out-of-plane direction, as the magnetic field points to the out-of-plane direction.

Therefore “magnetic drag anisotropy” will generate *positive* elliptic flow v_2 for those low p_T heavy quarks.

A body of conventional study on heavy quark dynamics is based on isotropic drag coefficients. In those studies [40, 41, 42], there are some tensions in simultaneously describing the nuclear modification factor R_{AA} and the elliptic flow v_2 of open heavy flavors in the low p_T regime. If one tries to reproduce the experimentally measured R_{AA} which is not significantly suppressed in this regime (see Ref. [44] for a review), the estimate of resulting v_2 typically undershoots the experimental data. This is because, as pointed out in Ref. [39], R_{AA} and v_2 are tightly correlated; namely, when suppression of R_{AA} is moderate, the thermalization of heavy quarks takes a long time, meaning a significantly small v_2 of heavy quarks compared to that of the medium. A common assumption involved in such estimates is the isotropy of the drag coefficients. It is thus tempting to propose a new scenario for resolution of this issue, the so-called “heavy-flavor puzzle”, on the basis of the anisotropic drag coefficients $\eta_{\parallel} \ll \eta_{\perp}$ shown in the present work. As discussed in Sec. 6, the anisotropic drag force coefficient will be able to generate an additional positive contribution to the elliptic flow in the low p_T regime without significantly changing R_{AA} . While our discussion on the consequence of anisotropic drag force coefficients would apply to any microscopic mechanism which would induce $\eta_{\parallel} \ll \eta_{\perp}$, we indeed identified one such origin of the mechanism, namely the strong magnetic field. Quantitative study on the basis of the dynamical modeling discussed in Sec. 6 will be an interesting future work. Our results for η can be readily implemented in those computations.

As the last comment, “magnetic drag anisotropy” discussed here has a deep connection to non-dissipative nature of anomalous transport [45, 62, 63] and this connection deserves a further study. We leave those interesting directions for the future study.

Acknowledgments

We thank Yukinao Akamatsu, Koichi Murase, Jorge Noronha, Hiroshi Ohno, Rob Pisarski, Alexander Rothkopf, Bjoern Schenke, and Sayantan Sharma for helpful discussions. K. F. is supported by JSPS KAKENHI Grant No. 15H03652 and 15K13479, K.H. is supported by JSPS Grants-in-Aid No. 25287066, and Y. Y. is supported by DOE Contract No. DE-SC0012704.

References

- [1] V. Skokov, A. Y. Illarionov and V. Toneev, *Int. J. Mod. Phys. A* **24**, 5925 (2009) [arXiv:0907.1396 [nucl-th]].
- [2] V. Voronyuk, V. D. Toneev, W. Cassing, E. L. Bratkovskaya, V. P. Konchakovski and S. A. Voloshin, *Phys. Rev. C* **83**, 054911 (2011) [arXiv:1103.4239 [nucl-th]].
- [3] A. Bzdak and V. Skokov, *Phys. Lett. B* **710**, 171 (2012) [arXiv:1111.1949 [hep-ph]].
- [4] W. T. Deng and X. G. Huang, *Phys. Rev. C* **85**, 044907 (2012) [arXiv:1201.5108 [nucl-th]].
- [5] D. E. Kharzeev, *Prog. Part. Nucl. Phys.* **75**, 133 (2014) [arXiv:1312.3348 [hep-ph]]; *Ann. Rev. Nucl. Part. Sci.* **65**, 0000 (2015) [arXiv:1501.01336 [hep-ph]].
- [6] J. Liao, *Pramana* **84**, 901 (2015) [arXiv:1401.2500 [hep-ph]].
- [7] V. A. Miransky and I. A. Shovkovy, *Phys. Rept.* **576**, 1 (2015) [arXiv:1503.00732 [hep-ph]].
- [8] X. G. Huang, arXiv:1509.04073 [nucl-th].
- [9] D. E. Kharzeev, L. D. McLerran and H. J. Warringa, *Nucl. Phys. A* **803**, 227 (2008) [arXiv:0711.0950 [hep-ph]]; K. Fukushima, D. E. Kharzeev and H. J. Warringa, *Phys. Rev. D* **78**, 074033 (2008) [arXiv:0808.3382 [hep-ph]].
- [10] D. E. Kharzeev and H. U. Yee, *Phys. Rev. D* **83**, 085007 (2011) [arXiv:1012.6026 [hep-th]].
- [11] G. M. Newman, *JHEP* **0601**, 158 (2006) [hep-ph/0511236].
- [12] Y. Burnier, D. E. Kharzeev, J. Liao and H. U. Yee, *Phys. Rev. Lett.* **107**, 052303 (2011) [arXiv:1103.1307 [hep-ph]].
- [13] E. V. Gorbar, V. A. Miransky and I. A. Shovkovy, *Phys. Rev. D* **83**, 085003 (2011) [arXiv:1101.4954 [hep-ph]].
- [14] A. A. Andrianov, V. A. Andrianov, D. Espriu and X. Planells, *Phys. Lett. B* **710**, 230 (2012) [arXiv:1201.3485 [hep-ph]].

- [15] K. Tuchin, Phys. Rev. C **87**, 024912 (2013) [arXiv:1206.0485 [hep-ph]].
- [16] G. Basar, D. Kharzeev, and V. Skokov, Phys. Rev. Lett. **109**, 202303 (2012) [arXiv:1206.1334 [hep-ph]].
- [17] K. Fukushima and K. Mameda, Phys. Rev. D **86**, 071501 (2012) [arXiv:1206.3128 [hep-ph]].
- [18] H. U. Yee, Phys. Rev. D **88**, no. 2, 026001 (2013) [arXiv:1303.3571 [nucl-th]].
- [19] K. Hattori, K. Itakura and S. Ozaki, arXiv:1305.7224 [hep-ph].
- [20] B. Muller, S. Y. Wu and D. L. Yang, Phys. Rev. D **89**, no. 2, 026013 (2014) [arXiv:1308.6568 [hep-th]].
- [21] Y. Yin, Phys. Rev. C **90**, no. 4, 044903 (2014) [arXiv:1312.4434 [nucl-th]].
- [22] K. Tuchin, Phys. Rev. C **88**, no. 2, 024911 (2013) [arXiv:1305.5806 [hep-ph]].
- [23] K. Tuchin, arXiv:1508.06925 [hep-ph].
- [24] L. McLerran and V. Skokov, Nucl. Phys. A **929**, 184 (2014) [arXiv:1305.0774 [hep-ph]].
- [25] N. Tanji, Annals Phys. **325**, 2018 (2010) [arXiv:1002.3143 [hep-ph]].
- [26] K. Tuchin, Adv. High Energy Phys. **2013**, 490495 (2013) [arXiv:1301.0099].
- [27] K. Fukushima, Phys. Rev. D **92**, 054009 (2015) [arXiv:1501.01940 [hep-ph]].
- [28] C. S. Machado, F. S. Navarra, E. G. de Oliveira, J. Noronha and M. Strickland, Phys. Rev. D **88**, 034009 (2013) [arXiv:1305.3308 [hep-ph]].
- [29] C. S. Machado, S. I. Finazzo, R. D. Matheus and J. Noronha, Phys. Rev. D **89**, 074027 (2014) [arXiv:1307.1797 [hep-ph]].
- [30] P. Gubler, K. Hattori, S. H. Lee, M. Oka, S. Ozaki, and K. Suzuki, arXiv:1512.08864 [hep-ph].
- [31] K. Marasinghe and K. Tuchin, Phys. Rev. C **84**, 044908 (2011) [arXiv:1103.1329 [hep-ph]].

- [32] J. Alford and M. Strickland, Phys. Rev. D **88**, 105017 (2013) [arXiv:1309.3003 [hep-ph]].
- [33] S. Cho, K. Hattori, S. H. Lee, K. Morita and S. Ozaki, Phys. Rev. Lett. **113**, 172301 (2014) [arXiv:1406.4586 [hep-ph]]; Phys. Rev. D **91**, 045025 (2015) [arXiv:1411.7675 [hep-ph]].
- [34] X. Guo, S. Shi, N. Xu, Z. Xu and P. Zhuang, Phys. Lett. B **751**, 215 (2015) [arXiv:1502.04407 [hep-ph]].
- [35] C. Bonati, M. D’Elia and A. Rucci, Phys. Rev. D **92**, 054014 (2015) [arXiv:1506.07890 [hep-ph]].
- [36] R. Rougemont, R. Critelli and J. Noronha, Phys. Rev. D **91**, 066001 (2015) [arXiv:1409.0556 [hep-th]].
- [37] D. Dudal and T. G. Mertens, Phys. Rev. D **91**, 086002 (2015) [arXiv:1410.3297 [hep-th]].
- [38] A. V. Sadofyev and Y. Yin, arXiv:1510.06760 [hep-th].
- [39] G. D. Moore and D. Teaney, Phys. Rev. C **71**, 064904 (2005) [hep-ph/0412346].
- [40] M. He, R. J. Fries and R. Rapp, Phys. Lett. B **735**, 445 (2014) [arXiv:1401.3817 [nucl-th]].
- [41] A. Beraudo, A. De Pace, M. Monteno, M. Nardi and F. Prino, Eur. Phys. J. C **75**, 121 (2015) [arXiv:1410.6082 [hep-ph]].
- [42] F. Scardina, S. K. Das, S. Plumari, J. I. Bellone and V. Greco, arXiv:1509.01551 [nucl-th].
- [43] Y. Akamatsu, Phys. Rev. C **92**, 044911 (2015) [arXiv:1503.08110 [nucl-th]].
- [44] A. Andronic *et al.*, arXiv:1506.03981 [nucl-ex].
- [45] K. Rajagopal and A. V. Sadofyev, JHEP **1510**, 018 (2015) [arXiv:1505.07379 [hep-th]].
- [46] S. Caron-Huot and G. D. Moore, Phys. Rev. Lett. **100**, 052301 (2008) [arXiv:0708.4232 [hep-ph]].

- [47] B. Feng, E. J. Ferrer and V. de la Incera, Phys. Rev. D **85**, 103529 (2012) [arXiv:1203.1630 [hep-th]].
- [48] K. Fukushima and Y. Hidaka, Phys. Rev. Lett. **110**, no. 3, 031601 (2013) [arXiv:1209.1319 [hep-ph]].
- [49] K. Hattori and K. Itakura, Annals Phys. **330**, 23 (2013) [arXiv:1209.2663 [hep-ph]].
- [50] J. Casalderrey-Solana and D. Teaney, Phys. Rev. D **74**, 085012 (2006) [hep-ph/0605199].
- [51] K. Fukushima, Phys. Rev. D **83**, 111501 (2011) [arXiv:1103.4430 [hep-ph]].
- [52] M. Le Bellac, *Thermal Field Theory*, (Cambridge University Press, 1996).
- [53] S. Mandelstam, Phys. Rev. D **11**, 3026 (1975).
- [54] A. V. Smilga, Phys. Lett. B **278**, 371 (1992).
- [55] K. Fukushima, J. Phys. G **39**, 013101 (2012) [arXiv:1108.2939 [hep-ph]].
- [56] J. I. Kapusta and C. Gale, *Finite-temperature field theory: Principles and applications*, (Cambridge University Press, 2006).
- [57] J. S. Schwinger, Phys. Rev. **125**, 397 (1962); Phys. Rev. **128**, 2425 (1962).
- [58] K. Hattori and K. Itakura, Annals Phys. **334**, 58 (2013) [arXiv:1212.1897 [hep-ph]].
- [59] R. Baier and E. Pilon, Z. Phys. C **52**, 339 (1991).
- [60] K. Hattori, K. Itakura, S. Ozaki and S. Yasui, Phys. Rev. D **92**, no. 6, 065003 (2015) [arXiv:1504.07619 [hep-ph]].
- [61] S. Ozaki, K. Itakura and Y. Kuramoto, arXiv:1509.06966 [hep-ph].
- [62] M. A. Stephanov and H. U. Yee, arXiv:1508.02396 [hep-th].
- [63] A. V. Sadofyev and Y. Yin, arXiv:1511.08794 [hep-th].